THE JOURNAL OF BIOLOGICAL CHEMISTRY VOL. 288, NO. 16, pp. 11407–11415, April 19, 2013

Impaired Intestinal Calcium Absorption in Protein 4.1R-deficient Mice Due to Altered Expression of Plasma Membrane Calcium ATPase 1b (PMCA1b)*

Received for publication, November 16, 2012, and in revised form, February 25, 2013 Published, JBC Papers in Press, March 4, 2013, DOI 10.1074/jbc.M112.436659

Congrong Liu[‡§], Haibao Weng[‡¶], Lixiang Chen[‡¶], Shaomin Yang[‡§], Hua Wang[‡§], Gargi Debnath[‡], Xinhua Guo[‡], Liancheng Wu[‡], Narla Mohandas[‡], and Xiuli An[‡¶1]

From the [‡]Red Cell Physiology Laboratory, New York Blood Center, New York, New York 10065, the [§]Department of Pathology, Peking University Health Science Center, Beijing 100191, China, and the [¶]Department of Bioengineering, Zhengzhou University, Zhengzhou 450051, China

Background: The function of protein 4.1R in small intestinal epithelia is unknown.
Results: 4.1R deficiency resulted in decreased expression of PMCA1b and impaired small intestinal calcium absorption.
Conclusion: Protein 4.1R plays an important role in small intestinal calcium absorption.
Significance: Our results identify a novel function for protein 4.1R and offer new insights into the mechanism of calcium absorption.

Protein 4.1R was first identified in the erythrocyte membrane skeleton. It is now known that the protein is expressed in a variety of epithelial cell lines and in the epithelia of many tissues, including the small intestine. However, the physiological function of 4.1R in the epithelial cells of the small intestine has not so far been explored. Here, we show that 4.1R knock-out mice exhibited a significantly impaired small intestinal calcium absorption that resulted in secondary hyperparathyroidism as evidenced by increased serum 1,25-$(OH)_2$-vitamin D_3 and parathyroid hormone levels, decreased serum calcium levels, hyperplasia of the parathyroid, and demineralization of the bones. 4.1R is located on the basolateral membrane of enterocytes, where it co-localizes with PMCA1b (plasma membrane calcium ATPase 1b). Expression of PMCA1b in enterocytes was decreased in $4.1^{-/-}$ mice. 4.1R directly associated with PMCA1b, and the association involved the membrane-binding domain of 4.1R and the second intracellular loop and C terminus of PMCA1b. Our findings have enabled us to define a functional role for 4.1R in small intestinal calcium absorption through regulation of membrane expression of PMCA1b.

Protein 4.1R was first identified as a component with an apparent molecular mass of 80 kDa on the red cell membrane. It plays an essential role in preserving the integrity of the cell during its lifetime in the circulation and in determining the complex system of interactions between the membrane skeleton and the transmembrane proteins (1, 2). Genetic studies have shown that a single 4.1R gene encodes a large repertoire of 4.1R isoforms by alternative mRNA splicing (3) and use of alternative promoters (4). The 4.1R isoforms are widely expressed in tissues and are located in a variety of subcellular compartments besides the plasma membrane (5). These include the nucleus (6), nuclear matrix (7), centrosome (8), and immunological synapse (9). In particular, it has been shown that 4.1R is expressed in many epithelial tissues (10, 11) and epithelial cell lines (12, 13). However, the function of 4.1R in these cells, particularly the function of 4.1R *in vivo*, remains largely unexplored. We have recently demonstrated that in stomach epithelial cells, 4.1R plays an essential part in linking cadherin-catenin complexes to the cytoskeleton through its direct interaction with β-catenin and also in ensuring the integrity of adherens junctions (11). The expression of 4.1R in the small intestine has also been reported (14), but its function in this context has not been established.

One major function of the small intestine is to absorb calcium. The intestine absorbs calcium by two mechanisms, active transcellular transport and passive paracellular transport (15). Transcellular Ca^{2+} transport is a multistep process, comprising entry of luminal Ca^{2+} into the enterocyte, followed by its translocation from the site of entry to the basolateral membrane and finally its extrusion from the cell into the circulation. In the mammalian small intestine, luminal Ca^{2+} entry involves TRPV6 (transient receptor potential vanilloid 6) in the apical region of the enterocyte (16–18). It is also known that calbindin-D9k, located in the cytoplasm, is responsible for translocation of Ca^{2+} from the apical to the basolateral region (19, 20). PMCA1b (plasma membrane calcium ATPase 1b), which is located at the basolateral membrane, is the principal Ca^{2+} extrusion protein in the small intestine (21).

We show here that 4.1R is expressed and co-localized with PMCA1b at the basolateral membranes of duodenal and jejunal epithelial cells and that the expression of PMCA1b is diminished in the absence of 4.1R. Importantly, 4.1R deficiency in mice results in impaired intestinal calcium absorption, which in turn leads to secondary hyperparathyroidism. These findings define a previously unidentified role for 4.1R in intestinal calcium absorption through its direct interaction with PMCA1b.

* This work was supported, in whole or in part, by National Institutes of Health Grants DK26263 and DK32094. This work was also supported by Grant 7082055 from Beijing Municipal Natural Science Foundation of China and Grant 81171905 from the Natural Science Foundation of China.
[1] To whom correspondence should be addressed: Red Cell Physiology Laboratory, 310 East 67th St., New York, NY 10065. Tel.: 212-570-3247; Fax: 212-570-3195; E-mail: xan@nybloodcenter.org.

MATERIALS AND METHODS

Generation and Use of 4.1R$^{-/-}$ Mice—The generation of 4.1R$^{-/-}$ mice has been described previously (22). The mice were backcrossed onto a C57BL/6 background for >10 generations. All mice were maintained at the animal facility of the New York Blood Center under pathogen-free conditions according to institutional guidelines. Animal protocols were reviewed and approved by the Institutional Animal Care and Use Committee. The mice were fed a normal diet containing 1.1% calcium, 0.8% phosphorus, and 0% lactose.

Preparation of Recombinant Proteins—Preparation of His-tagged 4.1R and its His-tagged 10-kDa spectrin-actin-binding domain was described previously (23, 24). The His-tagged 30-kDa membrane-binding domain of 4.1R (also called FERM domain) was cloned into the pET-31b(+) vector (Novagen, Madison, MI) using NsiI and XhoI sites (upstream and downstream, respectively). Maltose-binding protein-tagged lobes A–C were subcloned into the pMAL-c2X vector (New England Biolabs, Ipswich, MA) using EcoRI and SalI. His-tagged 16- and 22/24-kDa fragments of 4.1R were subcloned into the pET-28b(+) vector (Novagen) using NcoI and XhoI. Loop 1 of PMCA1b was subcloned into the pGEX-4T-2 vector using BamHI and SalI cloning sites. Loop 2 and the N and C termini of PMCA1b were subcloned into the pGEX-4T-2 vector using SalI and NotI cloning sites. The fidelity of all constructs was confirmed by DNA sequencing. The cDNA was transformed into *Escherichia coli* BL21(DE3) for protein expression. His-tagged 4.1R and its domains were purified on a nickel column, the GST-tagged PMCA1b fragments were purified on a glutathione-Sepharose 4B affinity column, and the maltose-binding protein-tagged recombinant proteins were purified on a maltose-binding column.

Generation of Anti-PMCA1b Antibodies—Anti-PMCA1b antibodies were raised in rabbits at Genemed Synthesis Inc. The antigens used for generating the antibodies were the GST-tagged recombinant loop 2 and C terminus of PMCA1b. The antibodies were affinity-purified on Affi-Gel 10 resin (Bio-Rad) coupled to the corresponding antigen. Initial characterization of the antibodies revealed that both antibodies recognized a 130-kDa gel band that was not detected when the antibodies were pre-absorbed with the corresponding antigen, demonstrating the specificity of the antibodies. As the two antibodies gave identical patterns, we chose anti-PMCA1b loop 2 antibody for the reported studies.

Immunoblot Analysis—Total protein from duodenal and jejunal epithelia was prepared as follows. Adult mice were killed, and the small intestines were rapidly removed and flushed with PBS containing protease inhibitor mixture (Sigma-Aldrich). Duodenal and jejunal mucosae were extracted and homogenized by sonication in 0.32 M sucrose, 0.01 M HEPES (pH 7.4), 2 mM EDTA, 1 mM DTT, and protease inhibitor mixture. The homogenate was spun at 900 × *g* for 5 min, and the supernatant proteins (20-μg samples) were analyzed on an 8% SDS-polyacrylamide gel and transferred to nitrocellulose membrane (Bio-Rad). The membranes were probed with rabbit anti-4.1R exon 13 or rabbit anti-PMCA1b loop 2 antibody, followed by HRP-conjugated goat anti-rabbit IgG (Jackson ImmunoResearch Laboratories). The film was developed using a Renaissance chemiluminescence detection kit (Pierce).

Immunohistochemistry—Paraffin-embedded tissue sections (4 μm thick) were dewaxed in xylene and rehydrated in descending concentrations of ethanol. Endogenous peroxidase activity was quenched with peroxidase-blocking reagent for 6 min. Sections were incubated overnight at 4 °C with rabbit anti-4.1R exon 13 antibody (1:50 dilution). After a thorough washing with PBS, the sections were treated with HRP-conjugated secondary antibody for 1 h at room temperature and developed with the liquid diaminobenzidine substrate chromogen system (DakoCytomation). Images were acquired with a Leica DM 2000 microscope.

Immunofluorescence—Mice were perfused with 4% paraformaldehyde, and the small intestines were dissected, embedded in optimal cutting compound (Sakura Finete U.S.A.), and snap-frozen in liquid nitrogen. Cryosections (6 μm thick) were cut in a cryostat, further fixed and treated with 4% paraformaldehyde and 0.1% Triton X-100 for 20 min at room temperature, and blocked with 10% horse serum and 1% BSA for 1 h at room temperature. The sections were incubated overnight at 4 °C with goat anti-4.1R exon 13 polyclonal antibody (1:100 dilution), followed by Alexa Fluor 488-conjugated donkey anti-goat IgGs (Molecular Probes). After blocking again, rabbit anti-PMCA1b loop 2 antibody (1:200 dilution) and Alexa Fluor 594-conjugated donkey anti-rabbit IgGs (Molecular Probes) were applied in sequence. Sections were mounted and observed under a Nikon Eclipse E600 epifluorescence microscope.

In Vivo Small Intestine $^{45}Ca^{2+}$ Absorption Assay—Ca^{2+} absorption was assessed by measuring serum $^{45}Ca^{2+}$ at early time points after oral gavage. Mice were fasted 12 h prior to the experiment, during which time they were hemodynamically stable under anesthesia (1.4 mg of urethane/g of body weight). The test solution contained 0.1 mM $CaCl_2$, 125 mM NaCl, 17 mM Tris, and 1.8 g/liter fructose and was enriched with 20 μCi/ml $^{45}CaCl_2$ (18 Ci/g; PerkinElmer Life Sciences). For the oral tests, 15 μl of this solution/g of body weight was administrated by gavage as described previously (25). Blood samples were obtained at specified time intervals. $^{45}Ca^{2+}$ in 10-μl aliquots of serum was measured by liquid scintillation counting.

Biochemical Assays—For blood analysis, blood was taken from the heart, and the serum was collected and stored at −80 °C until used. Serum calcium was measured with an Auto-Analyzer (Hitachi, Quebec, Canada). Mouse serum 1,25-$(OH)_2$-vitamin D_3 and parathyroid hormone (PTH)[2] levels were assayed using Gamma-B 1,25-dihydroxyvitamin D radioimmunoassay kits (IDS Inc.) and kits from Immunotopics, Inc. (San Clemente, CA) following the manufacturers' protocols. For bone calcium content assay, the right femur was dissected, freed of muscle and connective tissue, and then dried at 100 °C in an oven for 2 days. The dry weight was recorded. The bone was digested overnight in 2 ml of 10.5 mol/liter nitric acid. The solution was heated to 80 °C in a water bath, and 0.3 ml of 30% hydrogen peroxide was added. The volume was adjusted to 10 ml and filtered through Whatman No. 1 filter paper before

[2] The abbreviations used are: PTH, parathyroid hormone; PMCA, plasma membrane calcium ATPase.

measurement of calcium concentration, after appropriate dilution, using the QuantiChrom calcium assay kit (BioAssay Systems, Hayward, CA) according to the manufacturer's protocol.

Histological Examination of Parathyroid Glands—Tracheal blocks (containing the thyroid, parathyroid glands, trachea, and surrounding muscle and soft tissue) were extracted, fixed in 4% PBS-buffered formaldehyde for 24 h, processed, and embedded in paraffin wax. To examine the complete parathyroid glands, serial sections were cut to a thickness of 3.5 μm and processed for hematoxylin/eosin staining. To measure the parathyroid gland volume, 500–600 serial paraffin cross-sections of each tracheal block were examined by a pathologist, blinded as to the genotype and phenotype of the mice. Each specimen containing a whole cross-section of parathyroid gland was catalogued and measured in two orthogonal directions with a micrometer. The cross-section of greatest area and the sections defining the boundaries of the parathyroid gland were identified and used to calculate the volume according to the formula $a \times b \times c \times \pi/6$, where a, b, and c are the principal orthogonal dimensions (26). The volumes of the two glands were summed for each mouse.

Radiographic Analysis of Mouse Skeletal Structure—Radiographs were obtained by exposing euthanized mice to x-rays in a Faxitron pathology specimen x-ray cabinet. The animals were placed immediately above a fine-grained Polaroid 665 instant negative film package. Exposure was set at 20 kV for 35 s. The negatives were developed and printed according to the manufacturer's instructions.

RT-PCR Amplification of Plasma Membrane Calcium ATPases (PMCAs)—Total RNA was prepared from the small intestinal mucosa or brain using the RNeasy minikit (Qiagen) and was reverse-transcribed using the Superscript first-strand kit (Invitrogen) according to the manufacturers' instructions. Because the full-length transcripts of PMCAs are too long to amplify by standard PCR, two pairs of primers for each gene were used to amplify full-length PMCAs. The first pair of primers covered the region from exons 2 to 11, and the second pair from exons 11 to 21. Amplification of PMCA transcripts was carried out using AccuPrime *Taq* DNA polymerase (Invitrogen) according to the manufacturer's instruction. The PCR products of PMCA1b were sequenced at GENEWIZ, Inc. (South Plainfield, NJ).

Quantitative Real-time PCR of PMCA1b—Total RNA was extracted using the TRIzol reagent lysis method with the PureLink RNA minikit and purified with PureLink DNase (Invitrogen) according to the manufacturer's directions. Primers PMCA1FOR (TTAGAGAAGCCAGAATCAAGAAGT) and PMCA1REV (CAGCATCAGTGTCATCAATAAGG) were designed and provided by Primer Design Ltd. A single peak was seen in the melting curve, indicating primer specificity. PCR was performed as described previously (27). The abundance of PMCA1b message was normalized against GAPDH.

Co-immunoprecipitation of PMCA1b with 4.1R—The small intestinal mucosa from wild-type or $4.1R^{-/-}$ mice was lysed in ice-cold buffer containing 50 mM HEPES (pH 8.3), 420 mM KCl, 0.1% Nonidet P-40, 1 mM EDTA, 1 mM DTT, and protease inhibitor mixture for 30 min. The immunoprecipitation was performed as described previously (11). The membrane was probed with rabbit anti-4.1R exon 13 antibody or rabbit anti-PMCA1b loop 2 antibody.

Pulldown Assays—To examine the binding of 4.1R or its domains to PMCA1b, GST or the GST-tagged N terminus, loop 1, loop 2, or C terminus of PMCA1b was coupled to glutathione-Sepharose 4B beads at room temperature for 30 min. Beads were pelleted and washed. His-tagged 4.1R or 4.1R domains were added to the beads in a total volume of 100 μl. To examine the binding of PMCA1b fragments to subdomains (lobes A–C) of 30-kDa 4.1R, maltose-binding protein-tagged lobe A, B, or C was incubated with maltose-binding beads at room temperature for 30 min. After washing the beads, the GST-tagged loop 2 or C terminus of PMCA1b was added to the beads. The final concentration of both coupled protein and protein in solution was 1 μM. The mixture was incubated for 1 h at room temperature, pelleted, washed, and eluted with 10% SDS. The pellet was analyzed by 15% SDS-PAGE, and the protein brought down was detected by Western blotting using anti-His or anti-GST antibody.

Statistics—Data are expressed as means ± S.E. Statistical comparisons were evaluated by the t test. $p < 0.05$ was taken as statistically significant.

RESULTS

Expression and Localization of 4.1R in the Small Intestinal Epithelium—We and others have shown that 4.1R is widely expressed in epithelial cell lines and epithelial cells of various tissues, including the small intestine (10–14). To date, the function of 4.1R only in the epithelial cells of the stomach *in vivo* has been demonstrated (11). In this study, we focused on the small intestinal epithelia. We first examined the expression of 4.1R by Western blot analysis using anti-4.1R antibody, which targets the constitutive exon 13. Fig. 1*A* shows that the antibody revealed an ~110-kDa band in both the duodenal and jejunal epithelial cells of $4.1R^{+/+}$ mice, but not in those of $4.1R^{-/-}$ mice. Immunohistochemical staining using the same antibody showed that 4.1R was located predominantly at the basolateral membrane of epithelial cells of the duodenum (Fig. 1*B*, *left panel*) and jejunum (data not shown). No staining was observed in $4.1R^{-/-}$ duodenal epithelial cells (Fig. 1*B*, *right panel*).

Impaired Intestinal Calcium Absorption of 4.1R Knock-out Mice—The small intestine is responsible for absorption of various nutrients, including Ca^{2+}. Indeed, intestinal Ca^{2+} absorption plays a critical role in the regulation of Ca^{2+} homeostasis because it facilitates the entry of dietary Ca^{2+} into the extracellular compartment. Having shown that 4.1R is expressed in both the duodenum and jejunum, where active transcellular Ca^{2+} absorption takes place, we then compared the Ca^{2+} absorption in wild-type and 4.1R knock-out mice by gavage assay using $^{45}Ca^{2+}$ as a tracer. As shown in Fig. 2, the intestinal Ca^{2+} absorption was significantly impaired in 4.1R knock-out mice.

Biochemical Changes in $4.1R^{-/-}$ Mice—Because intestinal Ca^{2+} absorption is the critical step in the regulation of Ca^{2+} homeostasis, it is reasonable to speculate that the reduced intestinal Ca^{2+} absorption may lead to defective calcium homeostasis. To test this, we first measured the levels of serum 1,25-$(OH)_2$-vitamin D_3, PTH, and calcium. The results from 3-, 6-,

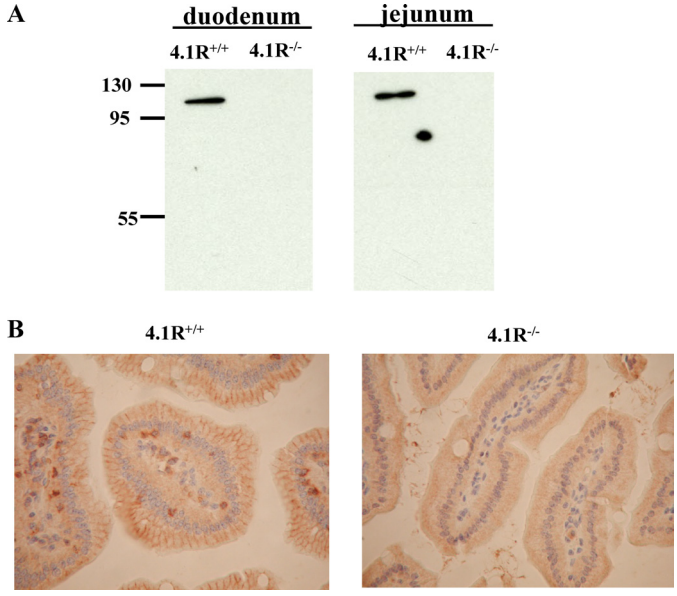

FIGURE 1. **Expression and localization of protein 4.1R on small intestinal epithelia.** *A*, Western blot analysis of 4.1R from the mucosa of the small intestine. Total cell lysates from $4.1R^{+/+}$ and $4.1R^{-/-}$ duodenal and jejunal mucosae were probed with anti-4.1R exon 13 antibody. Note the detection of an ~110-kDa band in $4.1R^{+/+}$ but not $4.1R^{-/-}$ samples. *B*, immunolocalization of 4.1R on enterocytes. $4.1R^{+/+}$ and $4.1R^{-/-}$ duodenal sections were stained with anti-4.1R exon 13 antibody. Note the staining of 4.1R on the basolateral membrane of enterocytes in $4.1R^{+/+}$ but not $4.1R^{-/-}$ duodenum.

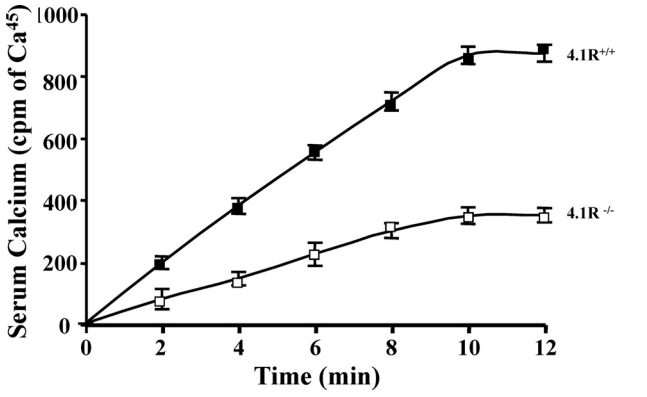

FIGURE 2. **Altered small intestinal calcium absorption in $4.1R^{-/-}$ mice.** Calcium absorption was assessed by lavage assay as described under "Materials and Methods." Note the significantly decreased uptake of calcium in $4.1R^{-/-}$ mice ($p < 0.01$, $n = 9$).

12-, and 18-month-old $4.1R^{+/+}$ and $4.1R^{-/-}$ mice are shown in Fig. 3. Fig. 3 (*A* and *B*) demonstrates that the increases in both 1,25-$(OH)_2$-vitamin D_3 and PTH levels were significant at all ages. Fig. 3*C* reveals a trend toward lower calcium levels in $4.1R^{-/-}$ mice, which became perceptible at 12 months and significant at 18 months. These findings strongly suggest that a secondary hyperparathyroidism occurs in $4.1R^{-/-}$ mice.

Hyperplasia of Parathyroid Glands of $4.1R^{-/-}$ Mice—To further confirm hyperparathyroidism, we performed histological examinations on parathyroid glands of wild-type and 4.1R-deficient mice. In all cases, four to six mice were examined. All $4.1R^{-/-}$ mice exhibited prominent parathyroid hypercellularity compared with their wild-type counterparts. Fig. 4*A* shows representative histological sections of $4.1R^{+/+}$ and $4.1R^{-/-}$ parathyroid glands, from which it is clear that the $4.1R^{-/-}$ parathyroid is much larger than the $4.1R^{+/+}$ parathyroid. Quantitative data from 3-, 6-, 12-, and 18-month-old mice are shown in Fig. 4*B*. It shows that the volumes of the glands of $4.1R^{-/-}$ mice were more than twice those of $4.1R^{+/+}$ animals.

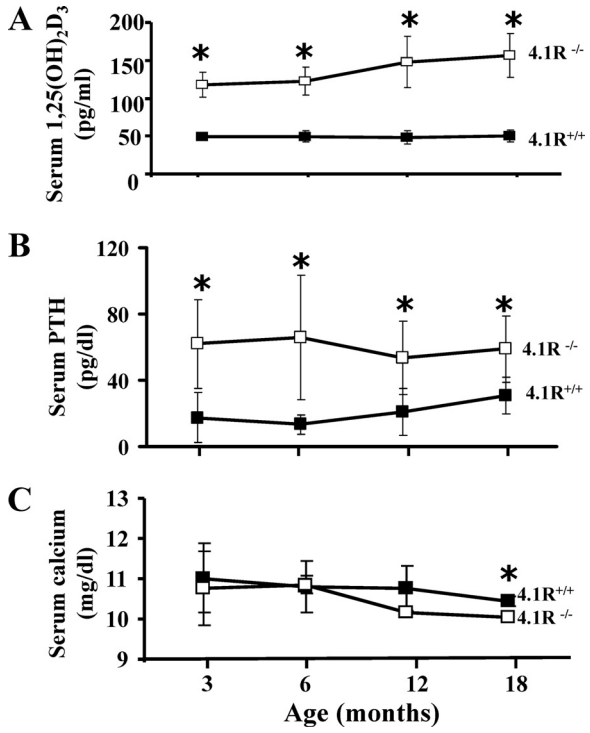

FIGURE 3. **Biochemical alterations in 4.1R knock-out mice.** The levels of serum 1,25-$(OH)_2$-vitamin D_3 (*1,25(OH)$_2$D$_3$*; *A*), PTH (*B*), and calcium (*C*) from 3-, 6-, 12-, and 18-month-old $4.1R^{+/+}$ and $4.1R^{-/-}$ mice were measured. Note the increased 1,25-$(OH)_2$-vitamin D_3 and PTH levels in all ages of $4.1R^{-/-}$ mice, but the decreased level of serum calcium in 18-month-old mice ($n = 9$). *, $p < 0.05$.

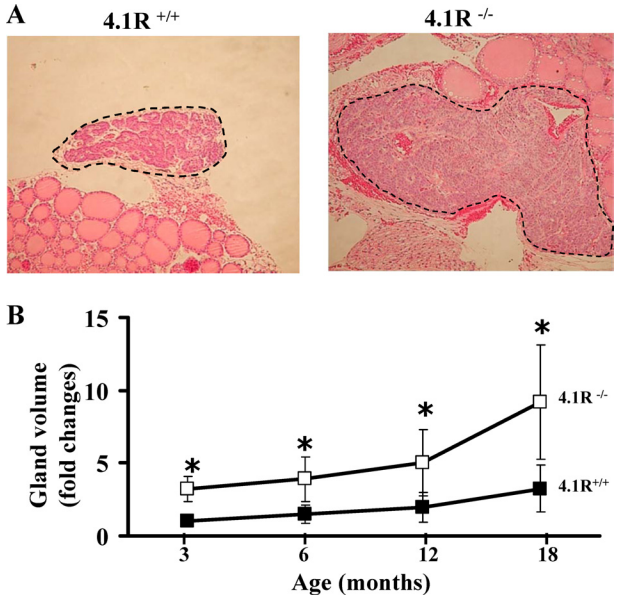

FIGURE 4. **Histological and pathological changes in $4.1R^{-/-}$ parathyroid glands.** *A*, representative hematoxylin/eosin staining of parathyroid glands from $4.1R^{+/+}$ and $4.1R^{-/-}$ mice. Note the marked enlargement and hypercellularity of the $4.1R^{-/-}$ parathyroid (20-fold) compared with its $4.1R^{+/+}$ counterpart. *B*, volumes of $4.1R^{+/+}$ and $4.1R^{-/-}$ parathyroid glands. Data from 3-, 6-, 12-, and 18-month-old $4.1R^{+/+}$ and $4.1R^{-/-}$ mice are plotted. *, $p < 0.05$. Note the increase in parathyroid gland volume at all ages.

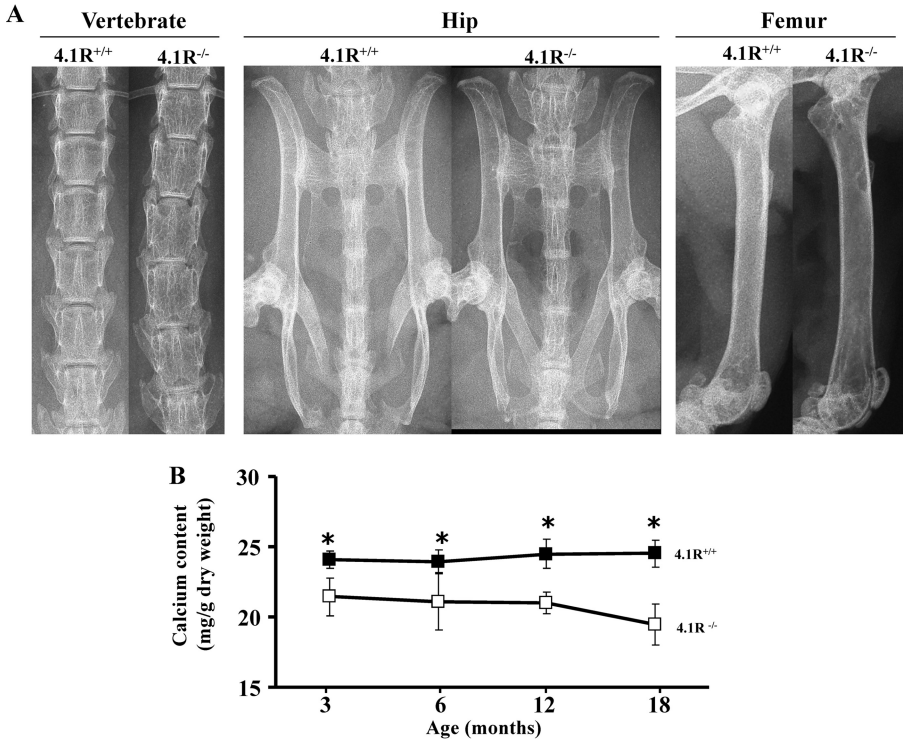

FIGURE 5. **Osteopenia in 4.1R$^{-/-}$ mice.** *A*, representative x-ray images of the skeletons of 4.1R$^{+/+}$ and 4.1R$^{-/-}$ mice. Images of vertebrae, hips, and femurs are shown. Note the decreased bone density in 4.1R$^{-/-}$ mice. Data are from a 1-year-old mouse. *B*, bone calcium content. Data from 3-, 6-, 12-, and 18-month-old 4.1R$^{+/+}$ and 4.1R$^{-/-}$ mice are plotted. *, $p < 0.05$. Note the decreased calcium content in 4.1R$^{-/-}$ mice at all ages.

Demineralization of the Skeleton in 4.1R$^{-/-}$ Mice—Having demonstrated the impairment of intestinal calcium absorption and the ensuing secondary hyperparathyroidism, we examined the bone density of the mice by x-ray radiography because both conditions can cause bone demineralization. The radiographs of the vertebrae, hips, and femurs of 4.1R$^{+/+}$ and 4.1R$^{-/-}$ mice (Fig. 5*A*) reveal a marked reduction in bone density in the latter. We also compared bone calcium contents in 3-, 6-, 12-, and 18-month-old wild-type and 4.1R$^{-/-}$ mice. In accordance with the reduced bone density, the calcium content in 4.1R$^{-/-}$ femurs was also significantly less (Fig. 5*B*).

PMCA1b Is Present in the Epithelium of the Mouse Small Intestine—Active transcellular small intestinal Ca^{2+} absorption involves extrusion of Ca^{2+} into the circulation from the basolateral membrane by PMCA (28). Mammalian PMCAs are encoded by four separate genes, and additional isoform variants are generated by alternative RNA splicing of the primary gene transcripts (28). To find which PMCA is present in the epithelium of the mouse small intestine, we analyzed the PMCA transcripts using a gene-specific primer set by RT-PCR. As the mRNAs of PMCA are >3 kb, we designed two primer sets for each gene to amplify the 5′- and 3′-portions separately with some overlap. Fig. 6*A* is a schematic representation of the primer selection. Fig. 6*B* shows that only PMCA1b fragments were amplified from the small intestinal epithelium. Sequence analysis of PMCA1b fragments revealed that the PMCA1b transcript contained all of the exons, thus identifying the isoform as PMCA1b. To ensure that the failure in the amplification of other PMCA transcripts was not due to the inability of the primers to function, we used the same primer sets to amplify these transcripts from brain. Fig. 6*C* shows that all PMCA brain transcripts were indeed amplified. Thus, PMCA1b is the isoform expressed in the mouse small intestinal epithelium.

Association of 4.1R with PMCA1b and Effect of 4.1R Deficiency on Expression of PMCA1b in Situ—As 4.1R is expressed at the basolateral membrane, we inferred that 4.1R may regulate intestinal calcium absorption through its interaction with PMCA1b. To test this, we first ascertained whether 4.1R and PMCA1b co-localize. Fig. 7*A* shows that this is the case, for both appeared on the basolateral membrane. We further performed co-immunoprecipitation assays to test for interaction between 4.1R and PMCA1b *in situ*. Fig. 7*B* shows that PMCA1b was co-precipitated with the 4.1R fragment by anti-4.1R antibody from 4.1R$^{+/+}$ (but not 4.1R$^{-/-}$) small intestine. It is well established that members of the protein 4.1 family serve as adaptors, linking transmembrane proteins to the cytoskeleton, and that lack of 4.1 proteins leads to loss or decreased expression of several transmembrane proteins (2, 11, 27). Therefore, we examined whether lack of 4.1R affects the expression of PMCA1b. Western blot analysis revealed that PMCA1b protein was indeed diminished in 4.1R$^{-/-}$ small intestine (Fig. 7*C*). To define the mechanism by which 4.1R loss leads to reductions in PMCA1b protein levels, we performed real-time PCR. Fig. 7*D* shows that there was no difference in PMCA1b transcript levels between 4.1R$^{+/+}$ and 4.1R$^{-/-}$ intestinal epithelial cells, implying that the reduced level of PMCA1b protein in 4.1R$^{-/-}$ cells is not due to reduced transcription. These results demonstrate that 4.1R is associated with PMCA1b *in situ* and that lack of 4.1R leads to reduced expression of PMCA1b protein, probably due to the instability of unattached PMCA1b.

Direct Binding of 4.1R to PMCA1b in Vitro—We further performed a series of pulldown assays to confirm the direct binding

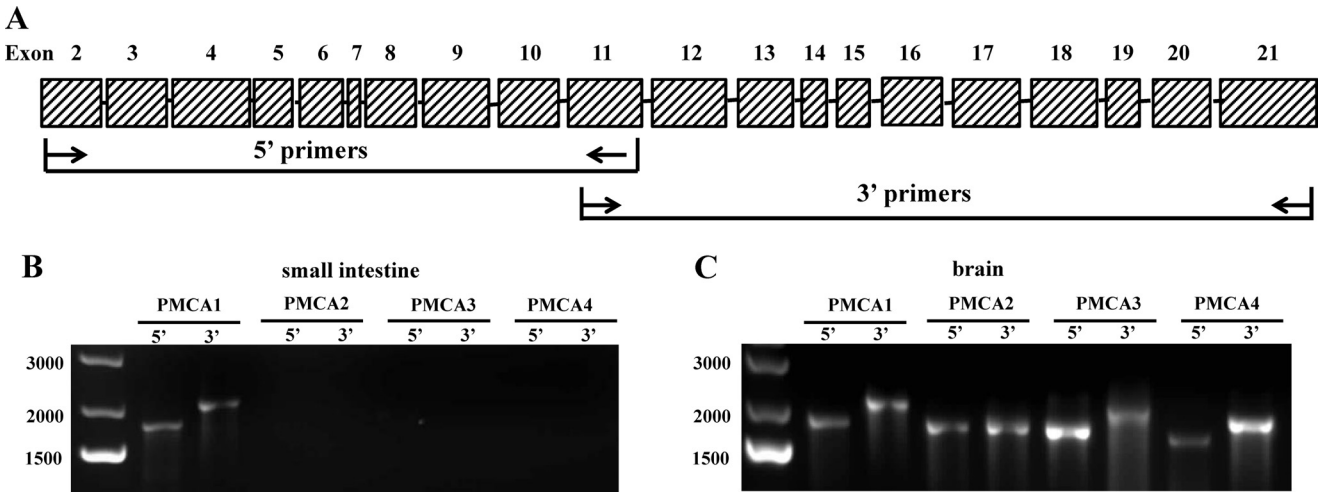

FIGURE 6. **RT-PCR analysis of PMCA transcripts.** *A*, schematic presentation of primer selection. *B*, amplification of PMCA transcripts from the small intestinal epithelium. The 5′- or 3′-portion of various PMCAs was amplified as described under "Materials and Methods" using cDNA from the small intestinal mucosa as a template. Note that only PMCA1b transcripts were amplified. *C*, amplification of PMCA transcripts from the brain. The 5′- or 3′-portion of various PMCAs was amplified as described for *B* using cDNA from the brain as a template. Note that all PMCA transcripts were amplified.

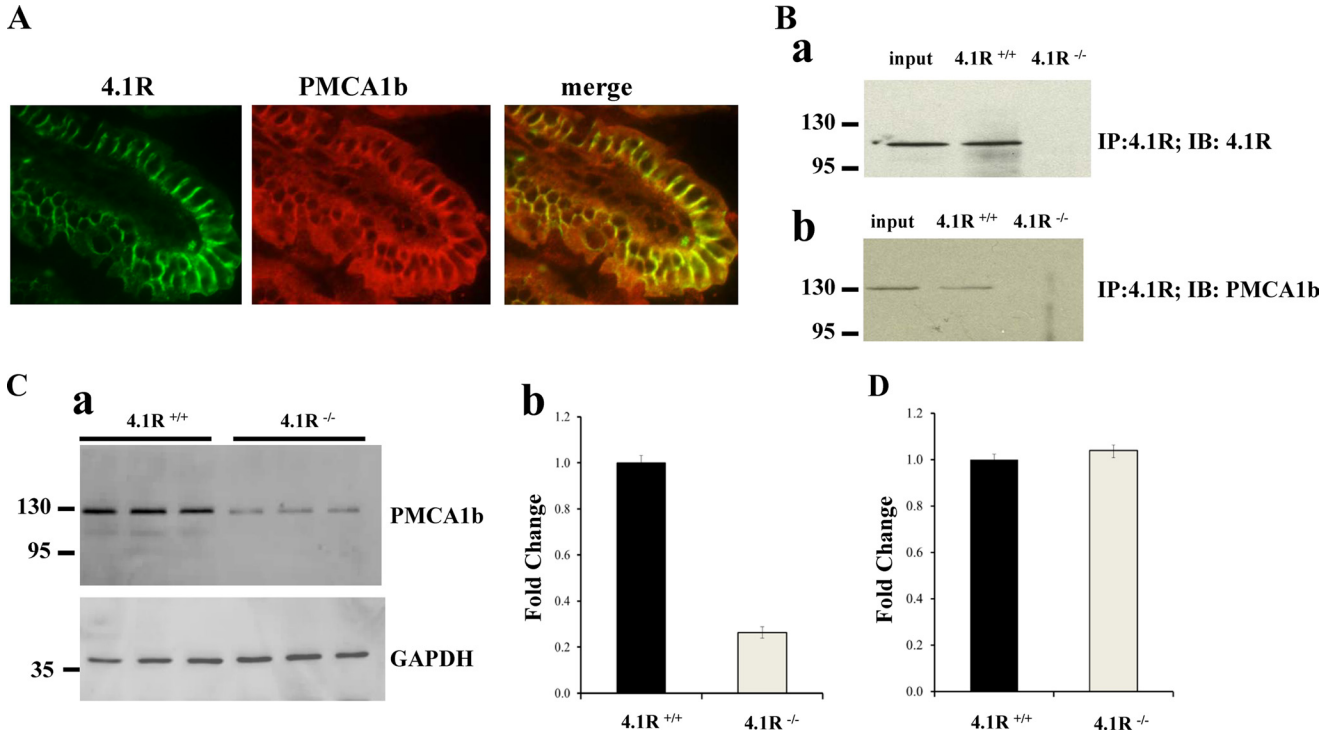

FIGURE 7. **Association of 4.1R with PMCA1b on enterocytes.** *A*, co-localization of 4.1R and PMCA1b. A section from a wild-type small intestine was co-stained with goat anti-4.1R exon 13 antibody (*green*) and rabbit anti-PMCA1b loop 2 antibody (*red*). Merged images show that 4.1R co-localized with PMCA1b on the bilateral membrane. *B*, co-immunoprecipitation of 4.1R with PMCA1b. The lysate from $4.1R^{+/+}$ or $4.1R^{-/-}$ small intestinal mucosa was immunoprecipitated (*IP*) by anti-4.1R IgG and detected by anti-4.1R antibody (*panel a*) or anti-PMCA1b loop 2 antibody (*panel b*), respectively. *IB*, immunoblot. *C*, Western blot analysis. 20 μg of total protein from three $4.1R^{+/+}$ or three $4.1R^{-/-}$ small intestinal mucosae was subjected to Western blotting using anti-PMCA1b loop 2 or anti-GAPDH antibody as shown in *panel a*, and the quantitative analysis is shown in *panel b*. *D*, quantitative real-time PCR, performed as described under "Materials and Methods." No significant difference was detected between $4.1R^{+/+}$ and $4.1R^{-/-}$ small intestines.

between 4.1R and PMCA1b. Fig. 8 (*A* and *B*) depicts the schematic models for 4.1R and PMCA1b, respectively. Fig. 8*C* shows that 4.1R bound to loop 2 and the C terminus of PMCA1b. Fig. 8*D* shows that 30-kDa membrane binding of 4.1R was responsible for the interactions with both loop 2 and the C terminus of PMCA1b. Furthermore, whereas loop 2 of PMCA1b bound to lobe A of the 30-kDa 4.1R domain, the C terminus of PMCA1b bound to lobe C (Fig. 8*E*). These findings demonstrate that 4.1R directly interacts with PMCA1b and that lack of 4.1R leads to impaired expression of PMCA1b.

DISCUSSION

Studies over the years have demonstrated that 4.1R is a multifunctional protein. However, most studies have been performed on cell lines, and the physiological function of 4.1R *in vivo* remains largely unexplored. To date, only the *in vivo* roles

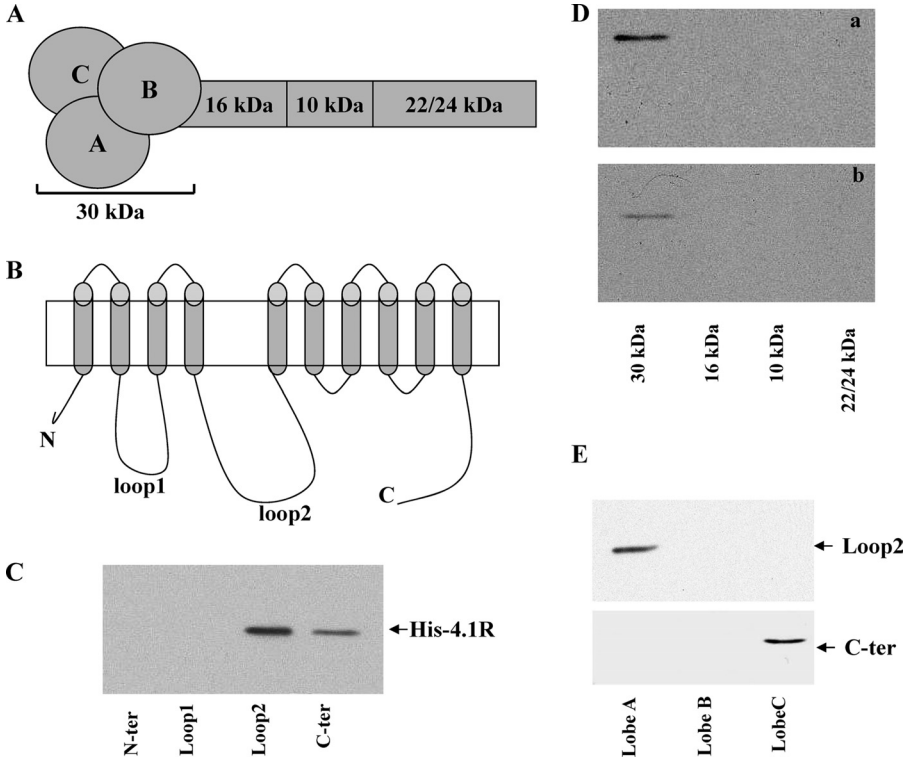

FIGURE 8. **Direct binding between 4.1R and PMCA1b *in vitro*.** *A*, schematic model of 4.1R structure. 4.1R contains four domains: the N-terminal 30-kDa membrane-binding domain, the 16-kDa domain, the internal 10-kDa spectrin-actin-binding domain, and the C-terminal 22/24-kDa domain. The 30-kDa domain consists of lobes A–C. *B*, schematic model of the PMCA1b structure. PMCA1b contains 10 membrane-spanning segments. Both the N and C termini are located on the cytosolic side of the membrane. In addition, a loop (designated loop 1 here) between transmembrane segments 2 and 3 and another large unit (designated loop 2 here) between transmembrane segments 4 and 5 are also facing the cytoplasmic side. *C*, binding of 4.1R to PMCA1b. Recombinant His-tagged 4.1R was incubated with GST-tagged fragments of PMCA1b. Binding was assayed by Western blotting using anti-His antibody for detection. Note the binding of 4.1R to loop 2 and the C terminus (*C-ter*) of PMCA1b. *N-ter*, N terminus of PMCA1b. *D*, binding of 4.1R domains to loop 2 and the C terminus of PMCA1b. His-tagged domains of 4.1R were incubated with the GST-tagged loop 2 or C terminus of PMCA1b. Binding was assayed as described for *C*. Note that only the 30-kDa domain bound to loop 2 and the C terminus of PMCA1b. *E*, binding of loop 2 or the C terminus of PMCA1b to subdomains of 30-kDa 4.1R. The GST-tagged loop 2 or C terminus of PMCA1b was incubated with maltose-binding protein-tagged lobes A–C of 30-kDa 4.1R. Binding was detected by Western blotting using anti-GST antibody. Note the binding of loop 2 to lobe A and the binding of C terminus to lobe C.

of 4.1R in regulating T cell function (9), in regulating repolarization and calcium handling in the heart (29), and in organizing adherens junctions in the stomach epithelia (11) have been documented using 4.1R knock-out mice. In the study, we have shown that 4.1R knock-out mice developed hyperparathyroidism and osteoporosis due to impaired intestinal calcium absorption. At the molecular level, we showed that lack of 4.1R resulted in decreased expression of PMCA1b. These findings have enabled us to identify an unexpected and novel role for 4.1R in regulating intestinal calcium absorption and thus calcium homeostasis through its direct interaction with PMCA1b.

It has been shown that 4.1R binds directly to a variety of transmembrane- or membrane-associated proteins. In erythrocytes, 4.1R associates with six membrane proteins and forms the core of the 4.1R-based macromolecular complex, and 4.1R deficiency in erythrocytes leads to the altered expression of the 4.1R-associated proteins (2). In $CD4^+$ T cells, 4.1R binds to the adaptor protein LAT (linker of activation of T cells) and inhibits the phosphorylation of LAT (9). In stomach epithelia, lack of 4.1R results in altered adherens junction formation due to the decreased expression of β-catenin (11). Here, we have shown that 4.1R directly bound to PMCA1b and that lack of 4.1R in enterocytes resulted in a significantly decreased expression of PMCA1b and the subsequent impairment of small intestinal calcium absorption. Taken together, these findings imply a general role for 4.1R in membrane protein-mediated functions by affecting the expression or function of these proteins.

It addition to 4.1R, we have recently demonstrated that lack of protein 4.1G, a member of the protein 4.1 family, leads to the decreased expression of the cell adhesion molecule nectin-like 4 in testis (27). Thus, it seems that members of the protein 4.1 family play a role in maintaining the expression of transmembrane proteins. Although the possible mechanisms of action of protein 4.1 members in the expression of various transmembrane proteins have yet to be fully defined, our findings that the levels of transcripts are not altered suggest that members of the protein 4.1 family affect protein expression at the post-transcriptional level.

Another effect of 4.1R on its binding partners is to modulate their functions. For example, it has been shown that, in red cells, binding of 4.1R to band 3 affects the association of band 3 with ankyrin (30). In $CD4^+$ T cells, 4.1R binds to the adaptor protein LAT and inhibits the phosphorylation of LAT (9). In the heart, lack of protein 4.1R appears to impact the function of several ion transporters affecting cardiac electrophysiology (29). A particular feature of the PMCAs is that their functions are regulated by a number of different mechanisms. PMCAs can be activated by Ca^{2+}/calmodulin (31), acidic phospholipids (32), and serine/threonine phosphorylation (33). All of these

regulators exert their effects by interacting with the C-terminal regulatory domain of PMCA (34). In addition to the abovementioned post-translational modifications, it has been suggested that members of the heterotrimeric G protein family may directly bind to the C-terminal domain of PMCA and regulate its functions (35). Our finding that 4.1R binds to the C terminus of PMCA1b raises the possibility that 4.1R may regulate the function of PMCA1b.

Active epithelial transcellular calcium absorption is a well defined process. Although the roles of TRPV6 in Ca^{2+} entry, calbindin-D9k in translocation, and PMCA in extrusion have been well established, little information is available concerning other molecular players. Our finding that a deficiency in the adaptor protein 4.1R results in significantly impaired intestinal calcium absorption strongly suggests that many yet to be defined molecules may also play important roles in epithelial calcium absorption.

In addition to small intestinal epithelia, calcium absorption also occurs in other epithelial tissues, including the kidney, placenta, and mammary glands. It has been reported that 4.1R, 4.1B, and 4.1N are expressed in the kidney (10). We have determined that all members of the 4.1 family are expressed in mammary glands and placenta.[3] It will be interesting in future studies to examine whether 4.1 proteins play roles in kidney calcium absorption or in calcium transport in mammary glands or placenta during reproductive events.

REFERENCES

1. Tchernia, G., Mohandas, N., and Shohet, S. (1981) Deficiency of skeletal membrane protein band 4.1 in homozygous hereditary elliptocytosis. Implications for erythrocyte membrane stability. *J. Clin. Invest.* **68,** 454–460
2. Salomao, M., Zhang, X., Yang, Y., Lee, S., Hartwig, J. H., Chasis, J. A., Mohandas, N., and An, X. (2008) Protein 4.1R-dependent multiprotein complex: new insights into the structural organization of the red blood cell membrane. *Proc. Natl. Acad. Sci. U.S.A.* **105,** 8026–8031
3. Conboy, J. G., Chan, J., Mohandas, N., and Kan, Y. W. (1988) Multiple protein 4.1 isoforms produced by alternative splicing in human erythroid cells. *Proc. Natl. Acad. Sci. U.S.A.* **85,** 9062–9065
4. Parra, M. K., Gee, S. L., Koury, M. J., Mohandas, N., and Conboy, J. G. (2003) Alternative 5′ exons and differential splicing regulate expression of protein 4.1R isoforms with distinct N termini. *Blood* **101,** 4164–4171
5. Gascard, P., Lee, G., Coulombel, L., Auffray, I., Lum, M., Parra, M., Conboy, J. G., Mohandas, N., and Chasis, J. A. (1998) Characterization of multiple isoforms of protein 4.1R expressed during erythroid terminal differentiation. *Blood* **92,** 4404–4414
6. Krauss, S. W., Larabell, C. A., Lockett, S., Gascard, P., Penman, S., Mohandas, N., and Chasis, J. A. (1997) Structural protein 4.1 in the nucleus of human cells: dynamic rearrangements during cell division. *J. Cell Biol.* **137,** 275–289
7. de Cárcer, G., Lallena, M. J., and Correas, I. (1995) Protein 4.1 is a component of the nuclear matrix of mammalian cells. *Biochem. J.* **312,** 871–877
8. Krauss, S. W., Chasis, J. A., Rogers, C., Mohandas, N., Krockmalnic, G., and Penman, S. (1997) Structural protein 4.1 is located in mammalian centrosomes. *Proc. Natl. Acad. Sci. U.S.A.* **94,** 7297–7302
9. Kang, Q., Yu, Y., Pei, X., Hughes, R., Heck, S., Zhang, X., Guo, X., Halverson, G., Mohandas, N., and An, X. (2009) Cytoskeletal protein 4.1R negatively regulates T-cell activation by inhibiting the phosphorylation of LAT. *Blood* **113,** 6128–6137
10. Ramez, M., Blot-Chabaud, M., Cluzeaud, F., Chanan, S., Patterson, M., Walensky, L. D., Marfatia, S., Baines, A. J., Chasis, J. A., Conboy, J. G., Mohandas, N., and Gascard, P. (2003) Distinct distribution of specific members of protein 4.1 gene family in the mouse nephron. *Kidney Int.* **63,** 1321–1337
11. Yang, S., Guo, X., Debnath, G., Mohandas, N., and An, X. (2009) Protein 4.1R links E-cadherin/β-catenin complex to the cytoskeleton through its direct interaction with β-catenin and modulates adherens junction integrity. *Biochim. Biophys. Acta* **1788,** 1458–1465
12. Mattagajasingh, S. N., Huang, S. C., Hartenstein, J. S., and Benz, E. J., Jr. (2000) Characterization of the interaction between protein 4.1R and ZO-2. A possible link between the tight junction and the actin cytoskeleton. *J. Biol. Chem.* **275,** 30573–30585
13. Kang, Q., Wang, T., Zhang, H., Mohandas, N., and An, X. (2009) A Golgi-associated protein 4.1B variant is required for assimilation of proteins in the membrane. *J. Cell Sci.* **122,** 1091–1099
14. Parra, M., Gascard, P., Walensky, L. D., Snyder, S. H., Mohandas, N., and Conboy, J. G. (1998) Cloning and characterization of 4.1G (*EPB41L2*), a new member of the skeletal protein 4.1 (*EPB41*) gene family. *Genomics* **49,** 298–306
15. Hoenderop, J. G., Nilius, B., and Bindels, R. J. (2005) Calcium absorption across epithelia. *Physiol. Rev.* **85,** 373–422
16. Peng, J. B., Chen, X. Z., Berger, U. V., Vassilev, P. M., Tsukaguchi, H., Brown, E. M., and Hediger, M. A. (1999) Molecular cloning and characterization of a channel-like transporter mediating intestinal calcium absorption. *J. Biol. Chem.* **274,** 22739–22746
17. Peng, J. B., Chen, X. Z., Berger, U. V., Weremowicz, S., Morton, C. C., Vassilev, P. M., Brown, E. M., and Hediger, M. A. (2000) Human calcium transport protein CaT1. *Biochem. Biophys. Res. Commun.* **278,** 326–332
18. Zhuang, L., Peng, J. B., Tou, L., Takanaga, H., Adam, R. M., Hediger, M. A., and Freeman, M. R. (2002) Calcium-selective ion channel, CaT1, is apically localized in gastrointestinal tract epithelia and is aberrantly expressed in human malignancies. *Lab. Invest.* **82,** 1755–1764
19. Bronner, F., Pansu, D., and Stein, W. D. (1986) An analysis of intestinal calcium transport across the rat intestine. *Am. J. Physiol.* **250,** G561–G569
20. Christakos, S., Gabrielides, C., and Rhoten, W. B. (1989) Vitamin D-dependent calcium binding proteins: chemistry, distribution, functional considerations, and molecular biology. *Endocr. Rev.* **10,** 3–26
21. Freeman, T. C., Howard, A., Bentsen, B. S., Legon, S., and Walters, J. R. (1995) Cellular and regional expression of transcripts of the plasma membrane calcium pump PMCA1 in rabbit intestine. *Am. J. Physiol.* **269,** G126–G131
22. Shi, Z. T., Afzal, V., Coller, B., Patel, D., Chasis, J. A., Parra, M., Lee, G., Paszty, C., Stevens, M., Walensky, L., Peters, L. L., Mohandas, N., Rubin, E., and Conboy, J. G. (1999) Protein 4.1R-deficient mice are viable but have erythroid membrane skeleton abnormalities. *J. Clin. Invest.* **103,** 331–340
23. An, X. L., Takakuwa, Y., Manno, S., Han, B. G., Gascard, P., and Mohandas, N. (2001) Structural and functional characterization of protein 4.1R-phosphatidylserine interaction. Potential role in 4.1R sorting within cells. *J. Biol. Chem.* **276,** 35778–35785
24. Gimm, J. A., An, X., Nunomura, W., and Mohandas, N. (2002) Functional characterization of spectrin-actin-binding domains in 4.1 family of proteins. *Biochemistry* **41,** 7275–7282
25. Van Cromphaut, S. J., Dewerchin, M., Hoenderop, J. G., Stockmans, I., Van Herck, E., Kato, S., Bindels, R. J., Collen, D., Carmeliet, P., Bouillon, R., and Carmeliet, G. (2001) Duodenal calcium absorption in vitamin D receptor-knockout mice: functional and molecular aspects. *Proc. Natl. Acad. Sci. U.S.A.* **98,** 13324–13329
26. Giangrande, A., Castiglioni, A., Solbiati, L., and Allaria, P. (1992) Ultrasound-guided percutaneous fine-needle ethanol injection into parathyroid glands in secondary hyperparathyroidism. *Nephrol. Dial. Transplant.* **7,** 412–421
27. Yang, S., Weng, H., Chen, L., Guo, X., Parra, M., Conboy, J., Debnath, G., Lambert, A. J., Peters, L. L., Baines, A. J., Mohandas, N., and An, X. (2011) Lack of protein 4.1G causes altered expression and localization of the cell adhesion molecule nectin-like 4 in testis and can cause male infertility. *Mol. Cell. Biol.* **31,** 2276–2286
28. Strehler, E. E., and Zacharias, D. A. (2001) Role of alternative splicing in generating isoform diversity among plasma membrane calcium pumps. *Physiol. Rev.* **81,** 21–50

[3] C. Liu, H. Weng, L. Chen, S. Yang, H. Wang, G. Debnath, X. Guo, L. Wu, N. Mohandas, and X. An, unpublished data.

29. Stagg, M. A., Carter, E., Sohrabi, N., Siedlecka, U., Soppa, G. K., Mead, F., Mohandas, N., Taylor-Harris, P., Baines, A., Bennett, P., Yacoub, M. H., Pinder, J. C., and Terracciano, C. M. (2008) Cytoskeletal protein 4.1R affects repolarization and regulates calcium handling in the heart. *Circ. Res.* **103,** 855–863
30. An, X. L., Takakuwa, Y., Nunomura, W., Manno, S., and Mohandas, N. (1996) Modulation of band 3-ankyrin interaction by protein 4.1. Functional implications in regulation of erythrocyte membrane mechanical properties. *J. Biol. Chem.* **271,** 33187–33191
31. Elshorst, B., Hennig, M., Försterling, H., Diener, A., Maurer, M., Schulte, P., Schwalbe, H., Griesinger, C., Krebs, J., Schmid, H., Vorherr, T., and Carafoli, E. (1999) NMR solution structure of a complex of calmodulin with a binding peptide of the Ca^{2+} pump. *Biochemistry* **38,** 12320–12332
32. Brodin, P., Falchetto, R., Vorherr, T., and Carafoli, E. (1992) Identification of two domains which mediate the binding of activating phospholipids to the plasma-membrane Ca^{2+} pump. *Eur. J. Biochem.* **204,** 939–946
33. Dean, W. L., Chen, D., Brandt, P. C., and Vanaman, T. C. (1997) Regulation of platelet plasma membrane Ca^{2+}-ATPase by cAMP-dependent and tyrosine phosphorylation. *J. Biol. Chem.* **272,** 15113–15119
34. Di Leva, F., Domi, T., Fedrizzi, L., Lim, D., and Carafoli, E. (2008) The plasma membrane Ca^{2+}-ATPase of animal cells: structure, function and regulation. *Arch Biochem. Biophys.* **476,** 65–74
35. Armesilla, A. L., Williams, J. C., Buch, M. H., Pickard, A., Emerson, M., Cartwright, E. J., Oceandy, D., Vos, M. D., Gillies, S., Clark, G. J., and Neyses, L. (2004) Novel functional interaction between the plasma membrane Ca^{2+} pump 4b and the proapoptotic tumor suppressor Ras-associated factor 1 (RASSF1). *J. Biol. Chem.* **279,** 31318–31328